

Dielectric spectroscopy characterization of Na⁺ ion-conducting polymer nanocomposite system PEO–PVP–NaIO₄–TiO₂

Georgi B. Hadjichristov^{*,†}, Daniela G. Kovacheva[†], Yordan G. Marinov^{*,‡},
Daniela B. Karashanova^{†,§}, Todor E. Vlahov* and Nicola Scaramuzza[§]

^{*}Georgi Nadjakov Institute of Solid State Physics
Bulgarian Academy of Sciences

72 Tzarigradsko, Chaussee Blvd., BG-1784 Sofia, Bulgaria

[†]Institute of General and Inorganic Chemistry
Bulgarian Academy of Sciences

Acad. Georgi Bonchev Str., 11 bd., BG-1113 Sofia, Bulgaria

[‡]Institute of Optical Materials and Technologies
“Acad. Jordan Malinowski”, Bulgarian Academy of Sciences
Acad. Georgi Bonchev Str., bl., 109, BG-1113 Sofia, Bulgaria

[§]Dipartimento di Fisica, Università degli Studi della Calabria
Via P. Bucci, Cubo 33B, Rende (CS), IT-87036, Italy

^{*}georgibh@issp.bas.bg

Received 7 June 2023; Revised 6 August 2023; Accepted 26 September 2023; Published 31 October 2023

We studied the effect of titanium dioxide (TiO₂) nanoparticles (NPs) on dielectric behavior of Na⁺ ion-conducting salt-complexed polymer nanocomposite system formed from a binary polymer blend of poly(ethylene oxide) (PEO) and polyvinyl pyrrolidone (PVP), with the addition of both sodium metaperiodate (NaIO₄) at concentration 10 wt.% and TiO₂ NPs of size ~10 nm, at concentrations 1, 2, 3, 4 and 5 wt.%. Free standing nanocomposite PEO/PVP/NaIO₄/TiO₂ films (150 μm) were characterized at room-temperature by analyzing their complex electrical impedance and dielectric spectra in the range 1 Hz–1 MHz. At the concentration of 3 wt.% of TiO₂ NPs, both ion conductivity and dielectric permittivity of the PEO/PVP/NaIO₄/TiO₂ ion-conducting dielectrics reach an enhancement by more than one order of magnitude as compared to nanoadditive-free case.

Keywords: Dielectric properties; sodium-ion-polymer electrolyte systems; titanium dioxide (TiO₂) nanoparticles; nanocomposites; KWW model.

1. Introduction

Metal ion (Li⁺, Na⁺, K⁺, Mg²⁺, Zn²⁺, ...) -conductive solid polymer systems have been gaining substantial attention in modern science and technology. Their cutting-edge advancements are promising for energy storage and conversion devices for innovative biomedical, defense and commercial applications. For instance, portable electronics such as personal healthcare devices, wearable sensors, and implantable medical devices, flexible and roll-up displays, touch screens and foldable smartphones, as well as automotive applications.^{1–8} Currently, there is a continuous increase of the fabrication of novel polymer ion-conductive dielectric systems and their effective use in supercapacitors, fuel cells, energy storage devices, electrochromic devices, electrical- and dielectric-based sensors and dye-sensitized solar cells.^{9–14} Nowadays, in the search for the complementing of Li-ion battery technology, sodium (Na⁺) ion-based rechargeable battery technology is receiving extensive attention in both industrial and academic sectors due to high safety,

low cost and other significant advances.^{15–21} Accordingly, various efficient Na⁺ ion-conducting salt-complexed polymer dielectric systems have been investigated.^{22–25}

Further, the engineering of advanced multifunctional ion-conducting polymer nanocomposites (ICPNCs), where nanomaterials, e.g., nanoparticles (NPs), are introduced into the polymer matrix of ICPNCs, is of special interest since such dielectric materials can have enhanced properties. In relevant applications, the performance of ionic devices, such as rechargeable metal-ion batteries, can be significantly improved.^{26–31} The research on ICPNCs is prominently increasing as a multidisciplinary scientific field with promising results extended to energy harvesting and various industrial applications.^{32,33} In particular, investigations on ICPNCs with included Titanium Dioxide (TiO₂) NPs have become an interesting and prospective area of research primarily due to the attractive mechanical, thermal, electric and dielectric properties of such ICPNCs.^{34–38} ICPNC dielectric materials with incorporated TiO₂ NPs are of importance in ionic,

future electrochemical and integrated smart electrochromic devices, batteries and supercapacitors, electrochemical sensors, nano- and 'oxide' electronics and other advanced applications.^{39–43} Furthermore, unique polymer-based electrolyte inks containing nanoTiO₂ become very promising for 3D-print flexible microbattery fabrication using micro-stereolithography. Coupled with other active components (organic or inorganic), TiO₂ NPs can be very efficient and functional agents for such purposes. The designed and fabricated novel ICPNC systems with included TiO₂ are not only interesting as solid polymer electrolytes but also as dielectric materials having improved dielectric properties, in addition to their enhanced ionic conductivity.^{44–46}

It has been established, in particular, by research of ICPNCs based on poly(ethylene oxide) (PEO) (or various PEO-containing polymer blends) complexed with alkali metal salts at moderate concentrations, e.g., 10 wt.%, that the addition of few wt.% of TiO₂ NPs improves the ionic conductivity and mechanical stability of the produced ICPNCs due to the formation of a network promoted by interaction of TiO₂ NPs with the alkali salts and PEO chains.^{47,48} An enhancement effect has been reported for various sizes of TiO₂ nanofillers in ICPNCs, ranging from 3 nm to 21 nm.^{34,47–49} Moreover, for TiO₂-nanofilled ICPNCs, it has been obtained that the smaller TiO₂ NPs enhance more efficiently the ionic transport properties of ICPNCs due to enhanced interfacial interaction between the polymer matrix and TiO₂ NPs.^{34,38,47–49} Therefore, a positive effect is expected from TiO₂ fillers with particle size of about 10 nm on the dielectric properties of the alkali salt-complexed ICPNCs. In these complex organic–inorganic molecular systems, both electrical conductivity and dielectric properties are coupled and governed by the same factors driven by the applied electric field. It was found in some studies, that the effect of TiO₂ NPs on the transport properties of ICPNCs is negligible if their size is larger than 22 nm.⁴⁸

In this work, we study ICPNCs engineered from TiO₂ NPs (~10 nm in size) and two polymers: PEO and polyvinyl pyrrolidone (PVP). As an ion donor, the salt sodium metaperiodate (NaIO₄) at a concentration of 10 wt.% was complexed with the PEO/PVP polymer blend. We study how the Na⁺-ion conductivity and dielectric properties of films of PEO/PVP/NaIO₄/TiO₂ ICPNCs are changed when the concentration of embedded TiO₂ NPs is varied from 1 wt.% to 5 wt.%. In our previous studies, we obtained that such TiO₂ NPs included in the PEO/PVP/NaIO₄ polymer electrolyte synthesized in the same way, led to enhancement of both electrical conductivity and dielectric properties of PEO/PVP/NaIO₄/TiO₂ films produced at concentration of TiO₂ NPs up to 3 wt.%,^{50–54} but not at a higher concentration of TiO₂ NPs.^{53,54} Here, the effects of TiO₂ NPs are investigated and discussed in terms of dipolar reorganization (dipolar relaxation) in the examined ICPNCs upon external alternating-current (AC) electric field. To do this, we have applied complex electrical impedance and dielectric

spectroscopy—powerful measurement techniques for the investigation of frequency-dependent dielectric polarization and relaxation processes contributing to the complex dielectric permittivity of the materials. Our aim was to elucidate the cause for the reducing electrical conductivity and dielectric permittivity of the produced PEO/PVP/NaIO₄/TiO₂ films at TiO₂ nanofiller concentration above 3 wt.% (namely 4 wt.% and 5 wt.%), of importance for the practical application of these ion-conducting dielectric materials. To draw a conclusion about the relevant physical mechanism, results from impedance and dielectric spectroscopy were correlated with those obtained by microstructural characterization techniques.

2. Experimental

PEO/PVP/NaIO₄/TiO₂ ICPNCs were synthesized as a binary polymer blend of PEO and PVP (in a weight ratio of 70:30 wt.%), complexed with NaIO₄ at a concentration of 10 wt.% (found to be an optimized composition⁵⁵), and TiO₂ NPs (~10 nm sized) included at concentrations of either 1, 2, 3, 4, or 5 wt.%. Chemically-stable homogeneous free-standing films (150 μm-thick) of the studied ICPNCs, as well as PEO/PVP (w/w = 70:30) and PEO/PVP/NaIO₄ without TiO₂ NPs, were produced by conventional solution-casting technique.⁵¹ As in our previous studies,^{50,52} the structural analyses confirmed the successful synthesis of these complex systems, as well as the incorporation of TiO₂ NPs in the PEO/PVP polymer blend matrix. As evidenced by X-ray diffraction (XRD), the precursor TiO₂ (nanopowder) is in pure anatase crystalline phase. From XRD scans, the mean size of TiO₂ NPs estimated using Scherrer's formula was 12.58 nm ± 2.86 nm (the scaling coefficient was taken equal to 0.9).

XRD measurements were carried out at ambient temperature on a Bruker D8 Advance diffractometer (Bruker AXS GmbH, Karlsruhe, Germany) using CuKα radiation (λ = 1.5418 Å) and LynxEye solid-state detector. Powder XRD patterns were collected at a standard Bragg–Brentano focusing geometry over the Bragg's reflection angle 2θ range of 5°–80°, with a constant step of 0.02° 2θ and a counting time of 35 s per step. The phase composition was determined using Diffrac.EVA v.4 software and ICDD-PDF2 (2021) database. Evaluation of the mean coherent domain size was performed with Topas v.4.2 software (Bruker AXS GmbH).

The surface morphology of the produced PEO/PVP/NaIO₄/TiO₂ films was observed at ambient temperature by Scanning Electron Microscopy (SEM) using digitized Philips 515 microscope (Philips, Eindhoven, The Netherlands). In order to enhance the image contrast of visualized surfaces, Au–Pd alloy was sputtered and deposited over them by means of SC7620 Mini Sputter Coater (Quorum Technologies, Lewes, UK). SEM images were obtained in SEI-mode at 0° angle of incidence of the electron beam to the sample surface, and electron accelerating voltage of 8 kV. Transmission Electron Microscopy (TEM) was also employed to

characterize the microstructural properties of the PEO/PVP/ $\text{NaIO}_4/\text{TiO}_2$ nanocomposites. TEM inspection was performed with JEOL JEM 2100 instrument (JEOL Ltd., Tokyo, Japan). The working accelerating voltage was kept at 200 kV.

The frequency spectra of the electrical impedance of the prepared films were measured by high-precision impedance workstation SP-200 (Bio-Logic Science Instruments). The films were placed between two blocking electrodes of copper (diameter = 1 cm) thus forming a symmetrical cell. The amplitude of the AC voltage applied transversally to the films was $0.1 V_{\text{RMS}}$. The impedance spectra were recorded in the range of 1 Hz–1 MHz at room temperature, in our case 25°C . By the measurements, identical experimental conditions were kept for all samples.

3. Results and Discussion

3.1. Microstructural studies

3.1.1. XRD

The TiO_2 NPs used here as precursors have anatase-type crystal structure described by tetragonal symmetry within the Space Group $I4_1/amd$. The obtained unit cell parameters $a = 3.7865(3) \text{ \AA}$ and $c = 9.5101(8) \text{ \AA}$ are close to that reported in the literature.⁵⁶ The mean coherent domain size (crystallite size) calculated on the basis of the whole XRD pattern is $18.0(1) \text{ nm}$. The crystallite size within the $\langle 101 \rangle$ direction was determined to be $19.0(4) \text{ nm}$, while the size in the $\langle 020 \rangle$ direction is $19.2(1) \text{ nm}$. This observation means that the morphology of the TiO_2 nanocrystallites is only slightly different from the isometric one. Such features of the material can be due to the synthesis method.

Figure 1 presents the XRD patterns recorded for the films under study. The characteristic crystalline diffraction peaks of PEO are at diffraction angles (in terms of Bragg angle 2θ) of 19.2° (singlet) and 23.3° (multiplet) (Fig. 1(a)). They are assigned to the (120) and ((032) + (112)) crystal planes of the PEO monoclinic crystal structure.^{57–59} Besides these strong peaks, the diffractograms also observed additional well-defined peaks resulting in the addition of TiO_2 nanofiller. The strongest among them was observed at $2\theta = 17.7^\circ$ (Fig. 1(c)). This XRD peak can be associated with crystalline structure of PEO, and was attributed to the (1 -2 -1) crystal plane of PEO. Apparently, the presence of the diffraction peak at $2\theta = 17.7^\circ$ can be related to specific modifications of PEO crystalline structure due to interaction of TiO_2 NPs with PEO functional units.

The characteristic XRD peak of TiO_2 nanocrystallites (anatase) at $2\theta = 25.3^\circ$ was resolved only for the sample of PEO/PVP/ $\text{NaIO}_4/\text{TiO}_2$ with wt.% NPs of TiO_2 (this peak is shown with arrow in Fig. 1(g)). The XRD patterns obtained for both PEO/PVP/ NaIO_4 and PEO/PVP/ $\text{NaIO}_4/\text{TiO}_2$ salt-complexed composites do not demonstrate distinct characteristic diffraction peaks of the salt NaIO_4 . This indicates the

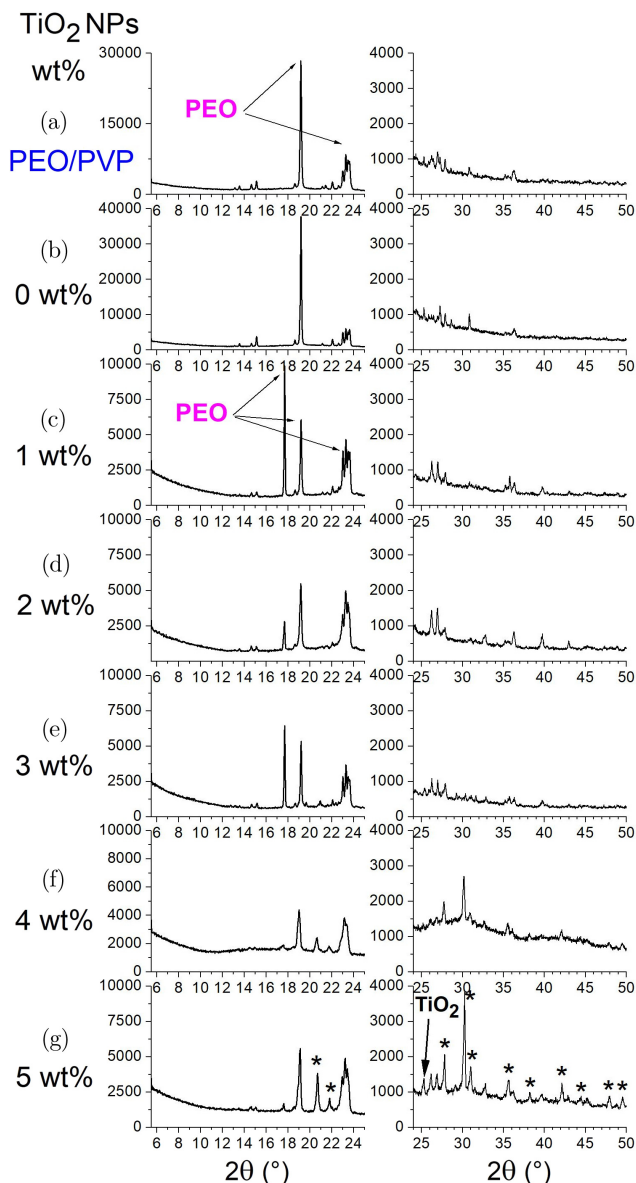


Fig. 1. XRD patterns recorded under the same experimental conditions for films of (a) PEO/PVP (w/w = 70 : 30%); (b)–(g) PEO/PVP/ $\text{NaIO}_4/\text{TiO}_2$ nanocomposites at denoted concentration of included TiO_2 NPs.

complete solvation of this ionic compound in the PEO/PVP polymer blend (due to interaction of NaIO_4 with functional groups of both polymers, PEO and PVP⁵⁵). In contrast, XRD pattern ascribed to sodium iodate (NaIO_3) were identified (indicated with asterisks in Fig. 1(g)). The strongest of them were at $2\theta = 20.66^\circ$, 21.85° , 26.3° , 27.8° and 30.25° . These peaks were most pronounced at the increasing percentage of TiO_2 nanofillers. This suggests that the compound NaIO_3 results from interactions induced by TiO_2 NPs. Most likely, this is TiO_2 NPs-assisted reaction during the synthesis of the PEO/PVP/ $\text{NaIO}_4/\text{TiO}_2$ nanocomposites and their drying at temperature 35°C .

Table 1. The unit cell parameters, the mean coherent domain size (ξ) of PEO in the polymer blend structure, and the degree of crystallinity (X_C) obtained from experimental data for: PEO; binary polymer blend PEO/PVP; PEO/PVP/NaIO₄ composite; PEO/PVP/NaIO₄/TiO₂ nanocomposites, at various concentration of TiO₂ NPs.

Sample	a (Å)	b (Å)	c (Å)	β (°)	ξ (nm)	X_C %
PEO	8.02(2)	13.15 (3)	19.33(4)	125.04(3)	31.1(5)	50.2
PEO/PVP	8.035(6)	13.129(9)	19.42(1)	124.93(2)	68(2)	26.8
PEO/PVP/NaIO ₄	8.041(2)	13.129(4)	19.427(8)	124.94(1)	89(1)	24.3
PEO/PVP/NaIO ₄	8.012(1)	13.063(2)	19.409(3)	124.996(7)	129(4)	19.1
+ 1 wt.% TiO ₂ NPs						
PEO/PVP/NaIO ₄	8.019(3)	13.073(6)	19.431(8)	125.02(1)	114(4)	20
+ 2 wt.% TiO ₂ NPs						
PEO/PVP/NaIO ₄	8.012(1)	13.068(2)	19.400(4)	124.962(8)	122(4)	15.8
+ 3 wt.% TiO ₂ NPs						
PEO/PVP/NaIO ₄	8.01(2)	13.12(3)	19.29(4)	124.96(4)	42(2)	10.6
+ 4 wt.% TiO ₂ NPs						
PEO/PVP/NaIO ₄	8.03(1)	13.17(2)	19.34(2)	124.82(3)	58(3)	14.5
+ 5 wt.% TiO ₂ NPs						

The changes in relative intensity of PEO XRD pattern with respect to the integral intensity of the broad background present in the XRD records in Fig. 1 were used to determine the crystallinity change of PEO/PVP/NaIO₄/TiO₂ nanocomposites as depending on the added TiO₂ NPs. The degree of crystallinity (X_C %) of the studied ICPNCs was calculated as the ratio of the total area under the PEO crystalline peaks to the total area under the diffractogram.^{55,59} The values of X_C are shown in Table 1. The results indicate that the addition of TiO₂ NPs leads to a suppression of crystallinity, i.e., it induces amorphization of the polymer host, a fact well-known for solid polymer nanocomposite electrolytes with added TiO₂ nanofiller.^{34–38,41–46} In the considered PEO/PVP/NaIO₄/TiO₂ ICPNCs, the TiO₂ nanofiller up to 5 wt.% improves the amorphous phase of semi-crystalline polymer blend PEO/PVP complexed with the salt NaIO₄.

The structural modification of the polymer PEO in the binary polymer blend PEO/PVP due to the included TiO₂ NPs can be characterized by calculations of the unit cell parameters and the mean coherent domain size (ξ) of PEO in the polymer blend structure. The values of the unit cell parameters for PEO obtained by fitting the whole XRD pattern profiles (without the lines of NaIO₃) (Table 1) are in good agreement with the literature data.⁶⁰ ξ obtained for PEO in the blend is about 68 nm (Table 1).

The addition of the salt NaIO₄ to the PEO/PVP blend leads to an increase in the crystallite size of the PEO constituent of the blend, due to the creation of additional bonds between Na⁺ ion and segments of PEO, in the process of formation of ion-polymer coordination complex during the synthesis of the samples. TiO₂ nanofiller of amount up to 3 wt.% does result in a further increase of the value of ξ , that implies a presence of additional interconnects with the PEO segments. Compared to PEO/PVP/NaIO₄, the values of parameters a , b and c of PEO in these samples of PEO/PVP/NaIO₄/TiO₂ slightly decrease, while β increases. With a

further increase of the concentration of the introduced TiO₂ NPs (4–5 wt.%), the values of the parameters a and β of PEO remain almost the same, b is increased, and c decreases. Importantly, such amounts of TiO₂ nanofiller resulted in considerable decrease of the value of ξ , which becomes even lower than that obtained for PEO/PVP/NaIO₄ without TiO₂. The results presented in Table 1 suggest that the included TiO₂ NPs induce a reorganization in the polymer crystalline structure of the synthesized PEO/PVP/NaIO₄/TiO₂ nanocomposites.

3.1.2. Electron microscopy (SEM and TEM)

Inspection by SEM showed that the included TiO₂ NPs significantly change the surface properties of the studied PEO/PVP/NaIO₄/TiO₂ films. Figure 2 shows representative examples of SEM micrographs of the surface of such films, as well as referent PEO/PVP and PEO/PVP/NaIO₄ films, obtained under the same experimental conditions, for comparison. In all cases, the observed morphology was characterized with inhomogeneity and randomly distributed defects of various sizes. The sample of PEO/PVP displayed the morphology (Fig. 2(a)) typical for this polymer blend composed with the semicrystalline PEO (70 wt.%) and amorphous PVP (30 wt.%), as prepared with solution casting.^{50,55,61,62} This sample possesses a complex microporous structure, which signifies its crystalline nature. Also, the surface morphology of such films is characterized with defects like craters of size ~ 10 – 50 μm , occurring at the last stage of the film preparation process (evaporation of methanol solvent during drying).

The microporous inhomogeneity of the PEO/PVP/NaIO₄ and PEO/PVP/NaIO₄/TiO₂ composite films produced at the same compositional ratio PEO:PVP = 70:30 wt.% and with the same solution-casting technique, was strongly reduced when the concentration of NaIO₄ was 10 wt.% (Fig. 2(b))

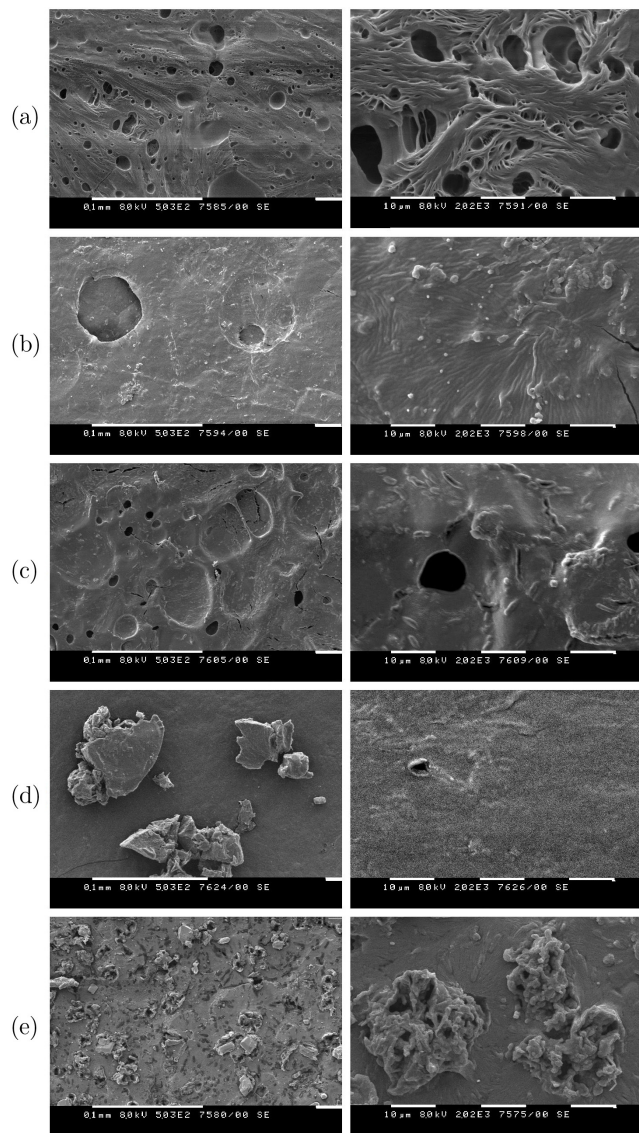


Fig. 2. SEM images at various magnifications showing surface view of films: PEO/PVP; (a) PEO/PVP/NaIO₄; (b) PEO/PVP/NaIO₄/TiO₂ at TiO₂ NPs concentration: (c) 1 wt.%, (d) 3 wt.% and (e) 5 wt.%.

(as reported also in Refs. 50, 55, 61 and 62), as well as with TiO₂ NPs added at concentration 1–3 wt.% (Figs. 2(c) and 2(d)) (reported in Refs. 50 and 52). Compared to PEO/PVP films, the surface topology of these composite films is quite different — their microstructure is denser and smoother, and microvoids (typical for crystalline structures) are considerably less. Such significant changes and more homogenized material are known to occur after cross-linking of polymer host by adding of other chemical component. The changes observed suggest that the formed composite material possesses a higher degree of amorphousness than PEO/PVP polymer blend, both prepared on identical way, i.e., the results obtained by XRD. This agrees with similar cases of reported effect of TiO₂ nanofiller in Na⁺-ion conducting PEO-based blended polymer electrolytes.⁴³

The surface smoothness of the salt-complexed PEO-PVP/NaIO₄/TiO₂ nanocomposite films drops at nanofiller concentration above 3 wt.% (Fig. 2(e)). In this case, solid microcreatures with relatively large dimensions (>10 μm) like crystallites. Most likely, they result from TiO₂ NPs that form aggregates, some of which are visible on the surface of the films. The dimensions of the aggregates reach 30 μm and more. Among these surface peculiarities and inhomogeneities, other microcrystallite formations can also be seen, such as the well faceted and prismatic-shaped structures in Fig. 2(e) probably due to the appearance of NaIO₃ compound (in accordance with the results and conclusions from the analysis of XRD data). Due to the low resolution of the scanning microscope, individual TiO₂ NPs were not distinguishable in the SEM images.

The morphology of TiO₂ NPs in the investigated PEO/PVP/NaIO₄/TiO₂ nanocomposites was visualized with TEM. In accordance with results obtained from XRD, TEM images display nearly round forms of the single TiO₂ NPs, optimally observed at a lower concentration of TiO₂ nanofillers, e.g., 1 wt.% (Fig. 3(a)). In micrographs taken at a low magnification (×10000) (Figs. 3(b) and 3(c)), well-separated nanosized aggregates of TiO₂ NPs within the continuous polymeric medium were clearly viewed. It can be noticed that these clusters have irregular shapes and different sizes. At higher concentrations of the nanofiller, e.g., in our case 3 wt.% (Fig. 3(d)) and 5 wt.% (Fig. 3(e)), an increase in the cluster sizes takes place. TEM images taken at a higher microscope magnification (×100000) (Figs. 3(f) and 3(g), respectively) confirm almost the circular shape of TiO₂ NPs and their sizes of the order of 10–15 nm.

3.2. Dielectric spectra

Figure 4 reports the real (Z') and imaginary (Z'') parts of the complex electrical impedance $Z^* = Z' + iZ''$ as a function of the frequency f of the AC electric field applied on the samples. It is seen that in contrast to the case at concentration 1 wt.% of TiO₂ NPs, the frequency behavior of the impedance of PEO/PVP/NaIO₄/TiO₂ films at a higher concentration of TiO₂ (≥ 2 wt.%) considerably differs from that of the NPs-free sample PEO/PVP/NaIO₄.

The maximum of Z'' corresponds to the value of the frequency $f_{\max Z''}$ at which the main dielectric active relaxation of the system occurs under the action of an AC electric field. The peak in the Z'' spectra originates from the orientation of the dipoles (the interplay between the resistance and the capacity of the samples). In our case, the $Z''(f)$ spectra in Fig. 4(b) suggest that as the percentage of TiO₂ NPs increases, the orientation of the dipoles becomes more complex. The maximum of Z'' is shifted towards the higher frequencies, from $f_{\max} \sim 10$ kHz up to 0.5 MHz, with a jump between the TiO₂ NPs values of 1 wt.% and 2 wt.%. At higher concentrations, up to 5 wt.%, the maximum of Z'' remains almost constant and this points towards saturation value. The

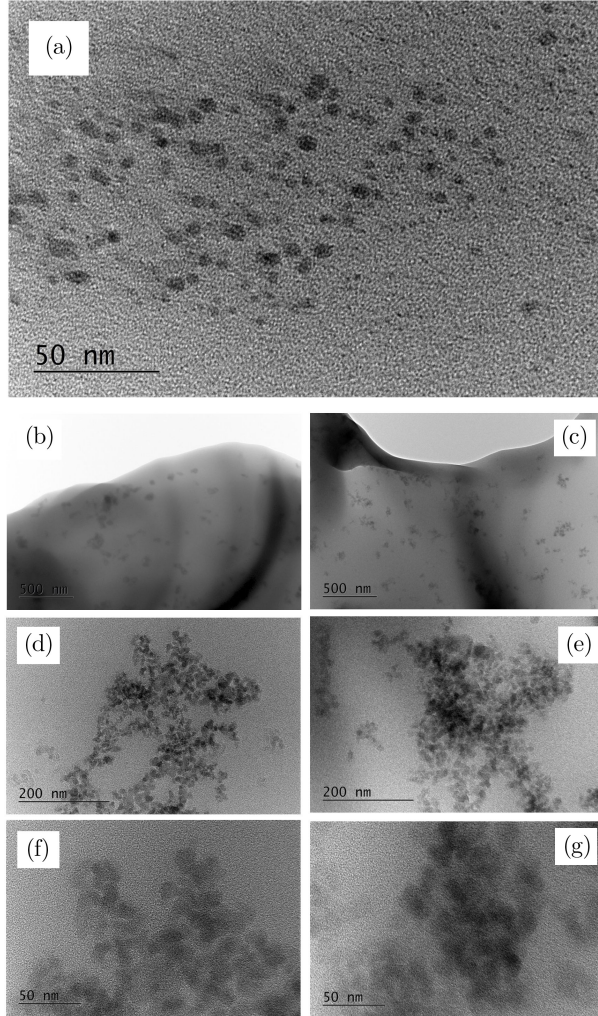


Fig. 3. TEM images of PEO/PVP/NaIO₄/TiO₂ nanocomposites. The concentration of TiO₂ NPs: ((a), (b)) 1 wt.%; ((d), (f)) 3 wt.% and ((c), (e), (g)) 5 wt.%.

observed shift of the Z'' peak means a decrease in the dielectric relaxation time. The observed saturation of the dielectric relaxation suggests that the presence of TiO₂ NPs at the concentration above 3 wt.% (in our case, 4–5 wt.%) in the polymer matrix is not favorable for the enhancement of polymer chain segmental motion.

The dielectric permittivity of the studied ICPNCs was determined as depending on the concentration of the TiO₂ nanofillers. Both quantities, the real (ϵ') and imaginary (ϵ'') parts of the complex dielectric permittivity function $\epsilon^* = \epsilon' - i\epsilon''$, are of significance for the ion conduction of polymer electrolytes. ϵ' represents the ability of the dielectric material to store energy in the electric field, and ϵ'' represents the energy lost as heat and dielectric leakage. In the polymer-ion electrolytes considered here, the polarization due to alignment of dipoles varies upon an applied oscillating electric field. The frequency-dependent relative ϵ' and ϵ'' were calculated from the acquired impedance spectra by using the

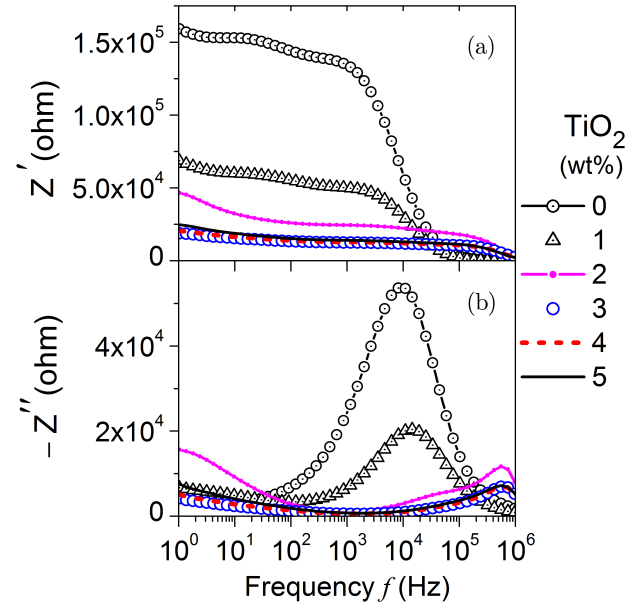


Fig. 4. Frequency spectra of real (a) and imaginary (b) parts of complex electrical impedance of PEO/PVP/NaIO₄/TiO₂ films at various concentrations of TiO₂ NPs.

relations

$$\epsilon' = \frac{-Z'' d}{2\pi f \epsilon_0 A |Z|^2} \quad \text{and} \quad \epsilon'' = \frac{Z' d}{2\pi f \epsilon_0 A |Z|^2}, \quad (1)$$

taking into account the values $A = 0.75 \text{ cm}^2$ and $d = 150 \mu\text{m}$ for the electrically active area and the film thickness, respectively. $\epsilon_0 = 8.85 \times 10^{-12} \text{ F}\cdot\text{m}^{-1}$ is the permittivity of free space. ϵ' and ϵ'' determine the stored and dissipated energy by conduction, respectively.

The variations of the permittivities ϵ' and ϵ'' with frequency f are shown in Fig. 5. For all samples, both ϵ' and ϵ'' functions exhibit large values at low frequency and were observed to monotonically decrease with the increase of f . Generally, the increase of ϵ' towards the lower frequencies can be ascribed to the retardation of the dipole oscillating frequency compared to the frequency of the applied electric field. As for ϵ'' , the reason for its decrease by increasing f is the high periodic reversal of the applied electric field. This variation is attributed to the tendency of dipoles in the macromolecules to orient themselves in the direction of the applied electric field in the low-frequency range. Conversely, their behavior is opposite at higher frequencies when the periodic reversal of the applied electric field is too fast and thus the dipoles and carriers cannot follow it. It is known that the sharp increase of dielectric permittivity at low frequency is related to the electrode polarization effect, which occurs due to the formation of electric double layers. These layers are built-up by the free charges at the electrolyte/electrode interface in a plane geometry.

The dielectric data are relevant to the superposition of two processes: A conductivity contribution (produces an increase of both ϵ' and ϵ'' on decreasing frequency) and a relaxation

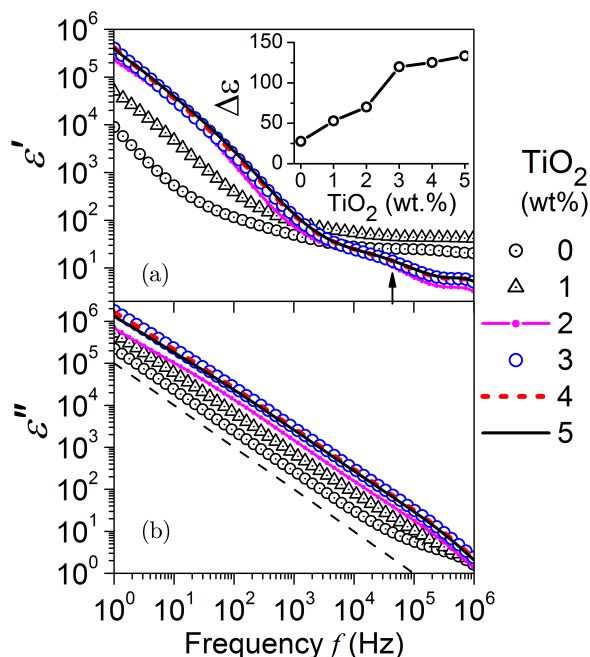


Fig. 5. Frequency spectra of real (a) and imaginary (b) parts of complex dielectric permittivity for PEO/PVP/NaIO₄/TiO₂ films. The inset in (a) shows a plot of dielectric relaxation strength $\Delta\varepsilon$ (at room temperature) versus the concentration of TiO₂ NPs. The dashed line in (b) illustrates the slope of f^{-1} function.

process exhibiting a maximum in ε'' frequency spectra. The TiO₂ NPs in the studied ICPNCs modify both these processes, as seen in corresponding dielectric behaviors. Like other polymer-based composites, the inclusion of TiO₂ nanoscale fillers leads to a change of the structure and chain dynamics of the polymer, and consequently of the dielectric properties of the ICPNCs.

As seen in Fig. 5, the addition of TiO₂ NPs at concentration 1–5 wt.% to PEO/PVP/NaIO₄ results in considerable increase of both ε' (at $f < 10$ kHz) and ε'' (in the range 1 Hz–200 kHz). Note that PEO is rated as a polymer with a low polarity. Below its melting temperature ($63 \pm 1^\circ\text{C}$), PEO exhibits values of ε' (decreasing with f) from $\varepsilon' = 6$ (at 10 Hz) to $\varepsilon' = 3.2$ (at 100 kHz) as measured at room temperature (23.5°C).⁶³ It should be also noted that significant contribution of the volumetric effect of TiO₂ NPs, with their higher intrinsic dielectric permittivity of about 100 (at 1 kHz) relies upon the preparation processes and the type of TiO₂ crystalline phase.^{64,65} Figure 5 shows that the variations of both ε' and ε'' follow one and the same trend with the increase of TiO₂ concentration. Detailed inspection of the double-logarithmic plots in Fig. 5(b) indicated a nearly linear decrease in $\varepsilon''(f)$ by increasing f , at TiO₂ content 0 and 1 wt%, suggesting that the power-law $\varepsilon''(f) \propto f^{-n}$ is fulfilled in a wide frequency range.

Because $n < 1$ (by fits on $\varepsilon''(f)$), n was found to be in the range 0.9–0.98) even in these two cases of low TiO₂ percentage (comparison in Fig. 5(b), the studied electrolyte

materials deviate from the ideal dielectric ($n = 1$ for ideal dielectric, with ideal (dipolar) Debye relaxation characterized by one relaxation time constant). A large deviation takes also place for the $\varepsilon''(f)$ plots at TiO₂ content 2–3–4–5 wt.% (Fig. 5(b)). In Fig. 5(a), no sizable relaxation was observed at TiO₂ concentration of 0 and 1 wt.%, while at TiO₂ concentration 2–5 wt.% a noticeable relaxation around the frequency $f \sim 20$ –40 kHz takes place (the corresponding feature is indicated by an arrow in Fig. 5(a)).

A reliable indicator of the change in the dipolar character of PEO/PVP/NaIO₄/TiO₂ due to variation in the concentration of incorporated TiO₂ NPs, may be the dielectric relaxation strength ($\Delta\varepsilon$). This quantity is a measure of dipole polarization. From the frequency-dependent ε' (Fig. 5(a)), we estimated $\Delta\varepsilon$ according to the relation $\Delta\varepsilon = \varepsilon'_s - \varepsilon'_\infty$, where ε'_s and ε'_∞ are the values of the static dielectric permittivity and the high frequency limiting dielectric permittivity, respectively.⁶⁶ One can assume that above 1 kHz the contribution of the electrode polarization process by the considered dielectric material is largely suppressed and the bulk material properties start to dominate in the contribution of dielectric polarization. On the other hand, ε' exhibits a leveling-off around 1 MHz (Fig. 5(a)). Hence, as a reasonable approximation in our case, one can take $\Delta\varepsilon = \varepsilon'(1 \text{ kHz}) - \varepsilon'(1 \text{ MHz})$.

The variation of $\Delta\varepsilon$ depending on the concentration of TiO₂ NPs is shown in the insert in Fig. 5(a). As seen, at the fixed concentration of the salt (NaIO₄ = 10 wt.%) in PEO/PVP/NaIO₄/TiO₂, the increase of the TiO₂ concentration leads to an enhancement of $\Delta\varepsilon$. The observed dielectric increment implies an enhanced electro-dipolar character of the system and an increase of polarization in the ICPNCs under discussion. Accordingly, the lowering of the slope of $\Delta\varepsilon$ dependence at higher content of TiO₂ (4 and 5 wt.%) is ascribed to diminution in polarization because the material becomes less dipolar. A probable cause for this may be some partial disorder induced by TiO₂ NPs in nanoscale vicinity at the polymer chains. Thus, the TiO₂ NPs included in the polymer matrix of PEO/PVP/NaIO₄/TiO₂ ICPNCs, due to their interaction with the polymer chains can affect the alignment of the electrical dipoles, e.g., those along the polymer chain directions. This effect is enhanced upon increasing amount of TiO₂. The restructuring of the PEO crystalline phase promoted by the TiO₂ nanofiller (evidenced by XRD, see Sec. 3.1.1) may affect the dipole polarization in the studied ICPNC films. Reorganization and/or disordering of molecular electrical dipoles (and even their possible breakdown) can result from formation of agglomerated structures of NPs. Such clusters are rather possible and were observed in the studied samples by TEM (see Sec. 3.1.2). Such effects of dipole reorganization, evidenced by dielectric and structural studies, have been reported for polymer nanocomposites based on PEO/PVP blend matrix nanofilled with TiO₂.³⁹

Analysis of dielectric permittivity spectra of the studied ICPNCs can be performed by use of Kohlrausch–Williams–Watts (KWW) model,^{67,68} expanded with the addition of

conductivity contribution present at lower frequencies. This approach is a generalization of the Debye relaxation model, with the following fitting function with two KWW terms:

$$\varepsilon''(f) = \frac{\sigma_{dc}}{\varepsilon_0(2\pi f)^n} + \text{F.T.} \left\{ \Delta\varepsilon_1 \exp \left[-\frac{t}{\tau_1} \right]^{\beta_1} + \Delta\varepsilon_2 \exp \left[-\frac{t}{\tau_2} \right]^{\beta_2} \right\}, \quad (2)$$

where the fit parameter σ_{dc} is the so-called ‘DC’ (direct current, static electric field, $f = 0$) electrical conductivity (i.e., the value of the real part of electrical conductivity at the hypothetical limit $f \rightarrow 0$), ε_0 is the vacuum permittivity, n is the power factor of the conductivity term, $\Delta\varepsilon$ are the dielectric strengths, β are the stretching exponents, τ are the dielectric relaxation times, t is the time variable, F.T. means the Fourier transform. It is well known that KWW function (stretched exponential) is proper to model the relaxations in heterogeneous systems of solid-state polymer dielectrics and is often applied for analysis of frequency-dependent dielectric permittivity data of solid-state polymer-containing systems and solid polymer electrolytes (composites and nanocomposites).^{69–71} The reason for the use of two KWW terms in Eq. (2) is the appearance of the small relative maximum in the impedance Z'' spectra (seen as a shoulder at about 50 kHz in Fig. 4(b)) at TiO₂ percentages 2–3–4–5 wt.%.

The Z'' spectra (Fig. 4(b)) exhibit a strongly perturbed dipole character of the PEO/PVP/NaIO₄/TiO₂ ICPNCs, and therefore, a deviation from the Debye’s model. For electrolytic polymer-based composite materials, it is well known that eutectic structures can be formed and hence two different characteristic times could be expected for the highly complex structures in the composite studied here. With the insertion of TiO₂ NPs, this type of dynamic structure is in some way deformed (slightly with 1 wt.% of TiO₂ and much more at higher percentages), and the dielectric properties of the considered material become more complex. The function in Eq. (2) cannot perfectly describe the microphases in PEO/PVP/NaIO₄/TiO₂ structure, but appropriate fits with physically acceptable fit parameters can be still obtained, as well as a reasonable dielectric permittivity value for the studied ICPNCs at the limit of the continuous.

By use of Eq. (2), the fits on ε'' dielectric spectral data for PEO/PVP/NaIO₄/TiO₂ were performed with LEVM complex nonlinear least-squares fitting and inversion program. Figure 6 illustrates the fits. They were best satisfying for the sample without TiO₂, and to some extent for the sample with 1 wt.% TiO₂. As the percentage of NPs increases, it was possible to obtain reasonable fits that give meaningful values only for the conductivity term. This implies that the effect from the inclusion of TiO₂ NPs is such that at their percentage > 1 wt.%, the possible characteristic modes of the PEO/PVP/NaIO₄/TiO₂ ICPNCs are suppressed by the displacement currents of the ions. Most likely this effect from TiO₂ is the

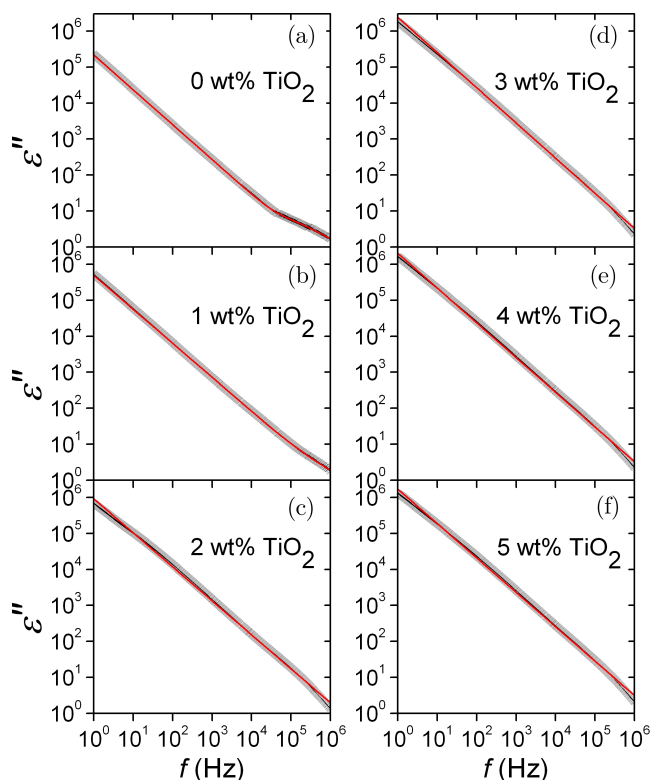


Fig. 6. (Color online) Frequency spectra of ε'' represented by the symbol (X); the red lines represent the best fits to the ε'' data with the use of fitting function from Eq. (2).

one expressed with a small relative maximum in Z'' spectra — the shoulder at about 50 kHz (Fig. 4(b)).

The values of σ_{dc} and n derived by the fits with Eq. (2) are shown in Fig. 7. The dependence of σ_{dc} on TiO₂ concentration (Fig. 7(a)) exactly matches the behavior for the ion conductivity obtained from the Z spectra (Nyquist impedance plots),⁵³ which is reasonable. The explanation of the increase of σ_{dc} is the synergetic effect due to high interfacial interactions between TiO₂ NPs and the functional units of polymers in the PEO/PVP polymer matrix.⁵⁰ On the other side, the diminishing of σ_{dc} is attributed to TiO₂–TiO₂ interactions that

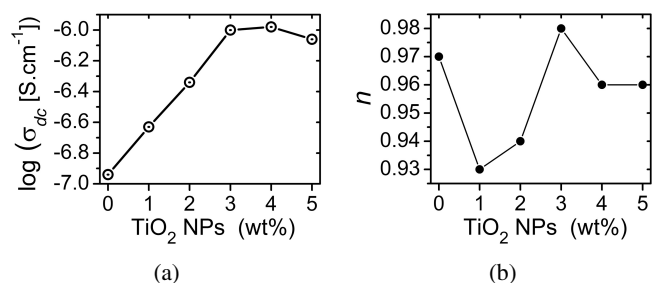


Fig. 7. Best-fit parameters obtained from the fits of ε'' data: Electrical conductivity σ_{dc} (a) and power factor n (b) versus the concentration of TiO₂ NPs.

are enhanced when the amount of TiO₂ NPs increases.⁵³ In this, a significant contribution has the clusterization of TiO₂ NPs (observed by TEM, see Sec. 3.1.2) that tends to increase with the increase of their concentration. As reported for similar TiO₂ NPs-modified salt-complexed ICPNC systems,^{35,36} the TiO₂ NPs clusterization leads to a decline of amorphous phase (observed by XRD in this work, by comparing the results for PEO/PVP/NaIO₄/TiO₂ samples at 4 wt.% and 5 wt.% TiO₂ NPs (recall Figs. 1(f) and 1(g) and Table 1), less ion-conducting pathways at the surface of the nanofillers, and probably to more immobilized polymer chains. A high content of TiO₂ NPs incorporated in the semicrystalline PEO/PVP polymer-blend matrix complexed with the ionic compound NaIO₄ does result in a weaker transport of the mobile Na⁺ ions, and therefore to a drop in ionic conductivity.^{45,53}

It has to be noted that such negative effect also takes place for the dielectric properties of PEO/PVP/NaIO₄/TiO₂ ICPNCs. Generally, the dielectric permittivity, the dielectric strength and dipole polarization, dielectric relaxation and dielectric loss tangent, (as well as the AC conductivity and electrical modulus) in such kind of complex ion-conducting polymer-ion coupled dielectric materials depend on the transport of the mobile (active) ions.^{35–37,41–46,72,73} Basically, there is no direct dependence. It depends on the particular system under investigation and there are only models that vary on a case-by-case basis.³⁷ In our case, the real and imaginary parts of complex dielectric permittivity could not be associated solely with the diffusion of mobile Na⁺ ions in the polymer matrix and ionic-related polarization mechanisms. Furthermore, apart from the frequency of the applied AC electric field, the dielectric response also depends on many other important factors, such as temperature, phase transitions and surface properties, whose effects are interrelated.

The trend in the variation of the power factor n versus the concentration of TiO₂ NPs (Fig. 7(b)) is near to the dependence of dielectric relaxation strength $\Delta\varepsilon$ on the concentration of TiO₂ NPs discussed above (Fig. 2(a)-the inset). This is reasonable because of the straightforward relevance between n and dielectric relaxation. As compared to the neat PEO/PVP/NaIO₄, the strong reduction of the value of the dimensionless parameter n is seen at 1 wt.% TiO₂ NPs (Fig. 7(b)). This can be interpreted as a jump deviation from a dielectric mode that is close to the single dielectric mode at a defined single frequency. The deviation can be considered as a specific spread of the single dielectric mode into various dielectric modes with corresponding characteristic frequencies.⁶⁹ Such alteration could be associated with the increase of the inhomogeneity (generally speaking) of the dielectric PEO/PVP/NaIO₄ due to the addition of nanoTiO₂.

The increasing behavior seen for n by increasing concentration of TiO₂ NPs (Fig. 7(b)) suggests an effect of dipole reorganization in a manner that a change in electrical conductivity is involved. Note that the inhomogeneity introduced

in the polymer-ion dielectrics does result in strong coupling between conductivity and dielectric relaxation (of dipoles in chain direction) at room temperature. The subsequent reduction of n by a further increase of TiO₂ concentration is associated again with the change in the dipolar character of the considered ICPNCs. This change is related to TiO₂ NPs-induced changes of both dipolar polarization and electrical conductivity in the ICPNCs.

3.3. Tangent loss

Additional analyses of ε' and ε'' functions can reveal further insights into the dielectric behavior of ICPNCs and how this behavior affects the performance of the ICPNCs, e.g., their ionic conductivity. Useful information about the ion transport in the studied ICPNCs PEO/PVP/NaIO₄/TiO₂ provides the frequency dependence of $\tan\delta$ calculated by expression:

$$\tan\delta = \varepsilon''/\varepsilon' = Z'/Z'' \quad (3)$$

$\tan\delta$ reflects the dielectric losses and is closely related to the process of dielectric relaxation (of dipoles) that controls the electrical conductivity. More commonly, $\tan\delta$ can be considered as the ratio of mobile-to-stored dipoles. As the dielectric strength $\Delta\varepsilon$ (discussed in Sec. 3.2), $\tan\delta$ depends on the characteristic properties of dipolar relaxation. Plots of $\tan\delta$ of the samples against the frequency f are shown in Fig. 8.

The loss spectra exhibit a broad peak at a certain frequency. This confirms the presence of relaxing dipoles in the studied ICPNCs. The loss-tangent relaxation time, $\tau_{\tan\delta}$, describes the polymer chain relaxation behavior and it is given by $\tau_{\tan\delta} = [2\pi f_{P(\tan\delta)}]^{-1}$. The dielectric polymer-chain relaxation time reflects the mobility of polymer chains. The results obtained for the examined ICPNCs (see the inset of Fig. 8) clearly indicate that $\tau_{\tan\delta}$ is a decreasing function of TiO₂ NPs concentration. This means that the inclusion of

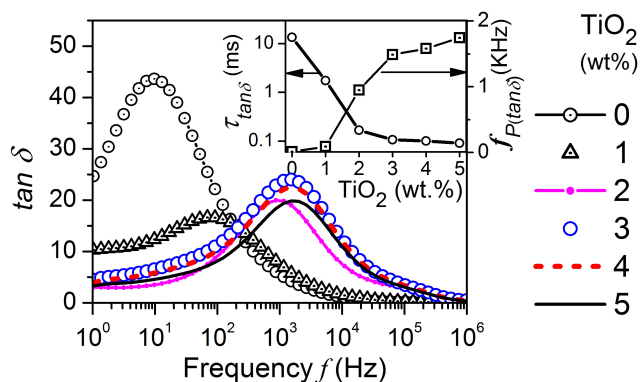


Fig. 8. Dielectric loss tangent ($\tan\delta$) as a function of frequency, as calculated by Eq. (3) for the studied PEO/PVP/NaIO₄/TiO₂ ICPNCs at various concentration of TiO₂ NPs. The inset shows the plots of the frequency $f_{P(\tan\delta)}$ corresponding to the maximum of the peak of $\tan\delta$, as well the polymer chain relaxation time $\tau_{\tan\delta}$, both versus TiO₂ percentage.

TiO₂ effectively leads to an increase of the segmental motion of the chains of PEO/PVP polymer matrix to which the Na⁺ cations are coordinated. For the ICPNCs investigated here, up to a concentration of 5 wt.% of TiO₂ NPs, this trend is continuous. Segmental motion of polymer chain facilitates the ion transport and thereby the ionic conductivity and dielectric properties would be improved.

4. Mechanism of TiO₂ NPs-Induced Modification of Ion Conductivity and Dielectric Response of PEO/PVP/NaIO₄/TiO₂ ICPNCs

In the studied PEO/PVP/NaIO₄/TiO₂ ICPNC dielectrics (as well as for a plenty of other ICPNC systems), the improvement in the amorphous phase (discussed in Sec. 3.1.1, in relation to data obtained by XRD measurements) and flexibility of the polymer network is known to be enhanced by high interfacial interactions of the nanoadditives with the polymer chains, and via possible conformational changes.^{37,44,66,74} These effects lead to an increase in segmental motion of the polymer chains in the amorphous domain, which supports the mobility enhancement of the charge carriers. In this way, the ionic conductivity in amorphous rich ion-conducting polymer systems, such as the ICPNCs studied here, based on PEO/PVP polymer blend is increased.^{50,75,76} Accordingly, the enhanced ion mobility will influence the dielectric properties of the PEO/PVP/NaIO₄/TiO₂ ICPNC system, too.

In our case, the amorphicity in polymeric material increases due to interactions between PEO oxygen and TiO₂ active species in the process of the synthesis of PEO/PVP/NaIO₄/TiO₂ ICPNCs. In these interactions, nanointerface effects induced by PEO molecular units and the inorganic TiO₂ NPs, play a significant role.³⁷ The increase of the amorphous region in polymeric material due to incorporation of TiO₂ NPs within PEO/PVP/NaIO₄ ion-conducting polymer system becomes similar as the effect from complexation of Na⁺ ions with the functional units of both polymers PEO and PVP. In both cases, the effects can be explained in terms of Lewis acid–base interactions with polymer segments.^{35–37} The oxygen vacancies on the TiO₂ NP surface (as Lewis acid) coordinate with ether oxygen atoms of the PEO polymer chains (Fig. 9), thereby the PEO crystallization is hindered. Moreover, this could efficiently prevent the possible recrystallization in the considered PEO-based ICPNCs containing amorphous polymer PVP in the PEO/PVP blend. Thus, a higher amorphous fraction in PEO/PVP/NaIO₄/TiO₂ is produced (formation of amorphous or amorphous-rich domains) as confirmed by XRD, and particularly suggested by SEM (see Sec. 3.1).

It should also be noted that the TiO₂ NPs compete with Na⁺ cations as Lewis acid in the formation of polymer-salt coordination complexes. This effect is enhanced at a higher

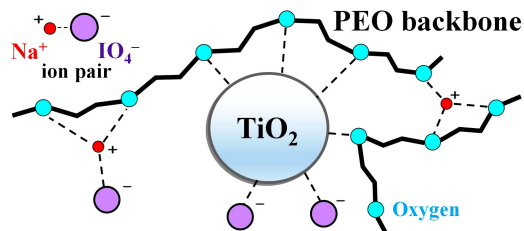


Fig. 9. Schematic illustration of the mechanism of the interaction between PEO/PVP/NaIO₄ ion-conducting polymer host and a TiO₂ NP guest.

concentration of TiO₂ NPs and may have contribution to the lowering of the ionic conductivity and dielectric permittivity measured for our films of PEO/PVP/NaIO₄/TiO₂ ICPNCs at 4–5 wt.% TiO₂ NPs. Further, the TiO₂ NPs can act as cross-linking centers for the polymer segments (Fig. 9), thereby modifying the polymer chain organization. A possible indicator of this effect may be the change in the mean coherence domain size (ξ) of polymer crystalline structure, as found by our XRD studies (see Sec. 3.1.1 and Table 1). Importantly, such a structural modification in the polymer host provides additional favorable conducting pathways for the Na⁺ ions at the high surface area of the TiO₂ NPs and thereby improves the Na⁺ ion transport. However, the clusters formed from TiO₂ NPs result in a decrease in the ion conductivity of PEO/PVP/NaIO₄/TiO₂ because of the unavailability of a part of the NPs as cross-linking centers for the ion-conducting polymer matrix. Also, nanofiller aggregation leads to localization of ions in the region of the cluster which reduces the numbers of the free ions for migration. In this case, the ion trapping effect may be due to high surface area of nanofiller. The effect of so generated space charges is negative for the ion transport because of the blockage of conduction paths provided by the polymer.^{35–38} Moreover, the higher concentration of cross-linking centers of TiO₂ NPs also plays negative role since they can promote a structure stiffness, i.e., the polymer chains become more immobilized, resulting in a decreasing ionic conductivity, as observed in this study at concentration of TiO₂ NPs above 4 wt.%. The above considerations for the TiO₂ NPs-induced modification apply to both ionic conductivity and the dielectric and dielectric-related properties of the PEO/PVP/NaIO₄/TiO₂ ICPNCs studied here (the dielectric permittivity, the dielectric strength and dipole polarization, dielectric relaxation and dielectric loss tangent) being closely related to Na⁺ ion transport in the PEO/PVP polymer blend complexed with the NaIO₄ salt.

On the other hand, in PEO/PVP/NaIO₄/TiO₂ ICPNCs the oxygen vacancies on the TiO₂ NP surface can also coordinate with oxygens from anions of NaIO₄ salt^{35–37} (this is also illustrated in Fig. 9). The interactions of Lewis acidic TiO₂ with the periodate IO₄⁻ anions lead to reduction of the ion pair (Na⁺:IO₄⁻) and release higher amounts of free Na⁺ ions. Together with the increasing amorphous phase, such effect

should further contribute to the enhanced ionic conductivity against the increase of the concentration of TiO_2 NPs, as observed here for the PEO/PVP/ NaIO_4 / TiO_2 samples with 1–3 wt.% TiO_2 NPs (recall Fig. 7(a)).

Besides the dissociation of undissociated salt into free ions by the interaction of TiO_2 NPs with the ionic compound NaIO_4 ,^{34,37} the TiO_2 NPs are capable to assist the reduction of NaIO_4 to iodate (NaIO_3). During the synthesis and preparation of our samples, this is concomitant, uncontrollable and inevitable. In fact, this effect was confirmed by the presence of the characteristic XRD pattern of NaIO_3 in the XRD records of PEO/PVP/ NaIO_4 / TiO_2 CPNCs, especially for the samples with 3–4–5 wt.% TiO_2 NPs (recall Fig. 1(g)).

Thus, like in similar TiO_2 NPs–modified ICPNCs,^{34–38,41,45–47} the interaction of TiO_2 NPs with PEO segments and ions of NaIO_4 induces structural modification of the polymer chains which provides favorable conditions and additional conduction path for faster migration of Na ion on the surface of the loaded TiO_2 NPs. The complex interplay between the above-mentioned processes of the Lewis acid–base interactions of TiO_2 NPs with PEO/PVP polymer blend and IO_4^- anions strongly depends on the concentration of TiO_2 NPs included within the polymer matrix. It is seen for the studied PEO/PVP/ NaIO_4 / TiO_2 dielectrics that the enhanced polymer chain segmental dynamics against the concentration of TiO_2 NPs is insufficient to increase the ion mobility if the concentration of TiO_2 NPs is relatively high (in our case when exceeds 4–5 wt.%). Other factors impose limitations on ion diffusion⁷⁷ and the addition of such content of nano TiO_2 does not provide the most suitable environment for ionic transportation, and thereby — for enhancement of ionic conductivity and dielectric properties considered here (dielectric permittivity and dipole polarization). Note in Fig. 8 that by increasing concentration of TiO_2 NPs 1–2–3 wt.% the level of $\tan\delta$ (the maximum of the $\tan\delta$ peak) increases, and at 4–5 wt.% it diminishes. This trend reflects the variations in both the strength of relaxation and the number of relaxing dipoles in the studied ICPNCs with the concentration of TiO_2 NPs.

Actually, the intensity of $\tan\delta$ peak and the corresponding frequency $f_{P(\tan\delta)}$ has a correlation with the diffusion coefficient of ions in the SPE material. In our case, $\tan\delta$ behavior suggests that at higher concentration of TiO_2 NPs, the localized dipolar and ionic motions are restricted. Indeed, the gradual reduction seen for values of $\tan\delta$ (Fig. 8) at 4–5 wt.% of TiO_2 NPs, indicates that the higher content of TiO_2 NPs leads to a hindrance of the polymer chain motion in PEO/PVP/ NaIO_4 / TiO_2 ICPNCs. However, the above-mentioned trend of reduction is also relevant to another process — the higher content of the loaded TiO_2 NPs induces nanostructural modification of the polymer segments resulting in less smooth and less sufficient conduction pathways at the high surface area of the NPs. Thus, a fast migration of Na^+ ions

through the ICPNC structure cannot be more ensured. In our view, at the increasing concentration of TiO_2 NPs the latter process is more responsible for the dielectric changes in considered ICPNCs, than the former one.

The situation for such nanofilled ion-conducting dielectrics is rather complicated because various processes are involved that affect the material properties. Finally, the inhomogeneities (at nano and microscale) in the composite systems, including also the grain boundaries of the electrode-specimen interfaces, are an important factor. In particular, the improvement of the surface topology upon the addition of TiO_2 NPs up to 3 wt.% (see Sec. 3.1.2) is beneficial for both conductivity and dielectric response of PEO/PVP/ NaIO_4 / TiO_2 film measured in plane-capacitor-like geometry, but they will be reduced by any nonregularities and inhomogeneity of both surfaces of the film. Upon addition of 3–5 wt.% TiO_2 nanofiller, the surface defects may be rather high due to formation of relatively large creatures at the film surface, as revealed SEM observations (Sec. 3.1.2). On the other hand, the inclusion of TiO_2 NPs leads to a very positive effect for the surface of the studied PEO/PVP/ NaIO_4 / TiO_2 solid salt-complexed polymer films — the lack of microvoids at the surface, as well as in the sub-surface region. Certainly, such property is very valuable, since it minimizes: (i) The possible ion trapping on the surface of such films, being in direct contact with electrodes where electric field is applied; (ii) interfacial polarization by real traps on the surface due to defects; (iii) space-charge limited conduction, as well as other unwanted processes at the film-to-electrode interface. As known, the ions captured by the interface traps can act as space charges. In general, such process by localized charge trapping should reduce the mobility of the charge carriers (in our case — the mobile Na^+ ions). Besides the Na^+ -ion conduction, the above considerations apply to the dielectric response of the PEO/PVP/ NaIO_4 / TiO_2 ICPNC films that also crucially depends on the quality and properties of the specimen-electrode interface. Furthermore, this issue is important for the possible dielectric applications of the ICPNCs investigated here.

Regardless of complexity of the physical mechanism, the conclusions deduced by the application of dielectric spectroscopy in the research of this kind of ICPNC systems are reliable. The results obtained here are consistent with the present knowledge on the effects from nanoadditives (in particular, TiO_2 NPs at reasonable concentrations) on the structure, morphology and the key properties of various ICPNC systems.

5. Conclusion

By means of macroscopic measurements with complex dielectric spectroscopy, the room-temperature dielectric permittivity and relaxation dynamics of salt-complexed ICPNCs

PEO/PVP/NaIO₄/TiO₂ were characterized as depending on the concentration of the included TiO₂ NPs (ranging from 1 wt.% to 5 wt.%). The results obtained indicate that 10 nm-sized TiO₂ NPs can significantly enhance both dielectric permittivity and Na⁺-ion conductivity of the investigated ICPNCs (at the polymer–blend–salt composition chosen here). The optimal concentration of TiO₂ NPs for this was found to be about 3 wt.%. A source of the positive effect on both ion conductivity and dielectric response is the interface across the polymer and nanometric TiO₂ additives. A change in dipolar polarization and relaxation behavior of the examined ICPNCs by adding TiO₂ NPs was evidenced, an effect commonly ascribed to TiO₂ nanosurface-induced interactions that also affect the ion conductivity.

The modification of the considered macroscopic properties of the studied ICPNCs due to the included TiO₂ NPs was linked to the corresponding complex atom/ion/nanoparticle interactions. Essentially, these interactions are controlled by the ether coordination site of PEO that makes this polymer polar. The inorganic TiO₂ nanofiller plays a dual role. By nanosurface interactions with functional groups of the PEO/PVP polymer blend and ionic inorganic salt NaIO₄, nanoTiO₂ enhances the dielectric and conductivity properties of ICPNCs PEO/PVP/NaIO₄/TiO₂. This effect, however, holds up to a particular percentage of TiO₂ NPs. At a concentration above 3 wt.%, the TiO₂ NPs act negatively and hinder the fast migration of Na⁺ ions via the PEO/PVP/NaIO₄/TiO₂ structure, thus reducing both the conductivity and dielectric properties.


Dielectric properties of the studied ICPNCs follow non-Debye type behavior. The results for the dielectric function and dynamic properties of the studied ion-dipolar-nanofiller electrolyte system support the previous reports that the incorporated TiO₂ NPs improve the amorphous phase of semi-crystalline polymer blend PEO/PVP complexed with the salt NaIO₄. Thus, TiO₂ NPs lead to enhancement of the polymer chains' flexibility. The dipolar and dielectric properties, as well as the relaxation behavior of polymer chains of PEO/PVP matrix are important factors for Na⁺-ion conduction. The information obtained on the change of dielectric behavior and ion conductivity due to included TiO₂ NPs will be useful for engineering and optimization of multifunctional materials based on plastic electrolytic systems with incorporated TiO₂ NPs for a variety of tasks, in which the dielectric response and conducting properties are central to manage their performance. They may be utilized in efficient Na⁺-ion batteries and other energy storage and conversion devices, as well as in other advanced energy and sensor systems and dielectric devices for applications in polymer electronics/ionics, sensorics and mechatronics.

Acknowledgments

We thank Dr. Hari Krishna Koduru from ISSP-BAS for providing us the ICPNC samples, as well as for the helpful discussions. Research equipment of Distributed Research


Infrastructure INFRAMAT, part of Bulgarian National Roadmap for Research Infrastructures, supported by Bulgarian Ministry of Education and Science was used in this investigation. This work was partially supported by the Ministry of Education and Science of Bulgaria (MESB), through the National Science Fund of Bulgaria (research project No. KP-06-N58/6/2021. Todor Vlachov gratefully acknowledges the support by the MESB under the National Research Programme, Young scientists and postdoctoral researches–2” approved by DCM 206/07.04.2022.


ORCID

Georgi B. Hadjichristov  <https://orcid.org/0000-0002-7141-3537>

Daniela G. Kovacheva  <https://orcid.org/0000-0002-1799-0851>

Yordan G. Marinov  <https://orcid.org/0000-0003-0616-7517>

Daniela B. Karashanova  <https://orcid.org/0000-0002-8785-3190>

Nicola Scaramuzza  <https://orcid.org/0000-0003-4847-6959>

References

- G. Qian, X. Liao, Y. Zhu, F. Pan, X. Chen and Y. Yang, Designing flexible lithium-ion batteries by structural engineering, *ACS Energy Lett.* **4**, 690 (2019).
- U.S. Army Research Laboratory, New lithium battery design could mean lighter, safer batteries for Soldiers, www.sciencedaily.com/releases/2019/09/190918100234.htm (2019).
- L. Qiao, X. Judez, T. Rojo, M. Armand and H. Zhang, Review — Polymer electrolytes for sodium batteries, *J. Electrochem. Soc.* **167**, 070534 (2020).
- D. Y. Voropaeva, S. A. Novikova and A. B. Yaroslavtsev, Polymer electrolytes for metal-ion batteries, *Russ. Chem. Rev.* **89**, 1132 (2020).
- X. Zhang, J. C. Daigle and K. Zaghbi, Comprehensive review of polymer architecture for all-solid-state lithium rechargeable batteries, *Materials* **13**, 2488 (2020).
- J. Lu, P. Jaumaux, T. Wang, C. Wang and G. Wang, Recent progress in quasi-solid and solid polymer electrolytes for multivalent metal-ion batteries, *J. Mater. Chem. A* **9**, 24175 (2021).
- Y. Zhao, L. Wang, Y. Zhou, Z. Liang, N. Tavajohi, B. Li and T. Li, Solid polymer electrolytes with high conductivity and transference number of Li ions for Li-based rechargeable batteries, *Adv. Sci.* **8**, 2003675 (2021).
- J. C. Barbosa, R. Gonçalves, C. M. Costa and S. Lanceros-Méndez, Toward sustainable solid polymer electrolytes for lithium-ion batteries, *ACS Omega* **7**, 14457 (2022).
- M. Yao, Q. Ruan, T. Yu, H. Zhang and S. Zhang, Solid polymer electrolyte with *in-situ* generated fast Li⁺ conducting network enable high voltage and dendrite-free lithium metal battery, *Energy Stor. Mater.* **44**, 93 (2022).
- Z. X. Huang, Z. H. Xie, Z. P. Zhang, T. Zhang, M. Z. Rong and M. Q. Zhang, Highly ionic conductive, self-healable solid polymer electrolyte based on reversibly interlocked macromolecule

- networks for lithium metal batteries workable at room temperature, *J. Mater. Chem. A* **10**, 18895 (2022).
- ¹¹J. O. Dennis, M. F. Shukur, O. A. Aldaghri, K. H. Ibnaouf, A. A. Adam, F. Usman, A. Alsadig, W. L. Danbature and B. A. Abdulkadir, A review of current trends on polyvinyl alcohol (PVA)-based solid polymer electrolytes, *Molecules* **28**, 1781 (2023).
 - ¹²D. Zhang, X. Meng, W. Hou, W. Hu, J. Mo, T. Yang, W. Zhang, Q. Fan, L. Liu, B. Jiang, L. Chu and M. Li, Solid polymer electrolytes: Ion conduction mechanisms and enhancement strategies, *Nano Res. Energy* **2**, e9120050 (2023).
 - ¹³N. Yazie, D. Worku, N. Gabbiye, A. Alemayehu, Z. Getahun and M. Dagne, Development of polymer blend electrolytes for battery systems: Recent progress, challenges, and future outlook, *Mater. Renew. Sustain. Energy* (2023).
 - ¹⁴A. Szczesna-Chrzan, M. Marczewski, J. Syzdek, M. K. Kochanec, M. Smoliński and M. Marcinek, Lithium polymer electrolytes for novel batteries application: The review perspective, *Appl. Phys. A* **129**, 37 (2023).
 - ¹⁵Pritam, A. Arya and A. L. Sharma, Dielectric relaxations and transport properties parameter analysis of novel blended solid polymer electrolyte for sodium-ion rechargeable batteries, *J. Mater. Sci.* **54**, 7131 (2019).
 - ¹⁶Z. Li, P. Liu, K. Zhu, Z. Zhang, Y. Si, Y. Wang and L. Jiao, Solid-state electrolytes for sodium metal batteries, *Energy Fuels* **35**, 9063 (2021).
 - ¹⁷H. Yin, C. Han, Q. Liu, F. Wu, F. Zhang and Y. Tang, Recent advances and perspectives on the polymer electrolytes for sodium/potassium-ion batteries, *Small* **17**, 2006627 (2021).
 - ¹⁸F. Gebert, J. Knott, R. Gorkin III, S. L. Chou and S. X. Dou, Polymer electrolytes for sodium-ion batteries, *Energy Storage Mater.* **36**, 10 (2021).
 - ¹⁹F. S. Genier, S. Pathreker, P. O. Adebo, P. Chando and I. D. Hosein, Design of a Boron-containing PTHF-based solid polymer electrolyte for sodium-ion conduction with high Na⁺ mobility and salt dissociation, *ACS Appl. Polym. Mater.* **4**, 7645 (2022).
 - ²⁰M. A. Jothi, D. Vanitha, N. Nallamuthu and K. Sundaramahalingam, Optical and dielectric characterization of biopolymer pectin based electrolytes with NaCl, *J. Elastom. Plast.* **54**, 800 (2022).
 - ²¹R. R. Gaddam and X. S. (George) Zhao, *Handbook of Sodium-Ion Batteries Materials and Characterization* (Jenny Stanford Publishing Pte. Ltd., Singapore, 2023).
 - ²²Q. Pan, D. Gong and Y. Tang, Recent progress and perspective on electrolytes for sodium/potassium-based devices, *Energy Storage Mater.* **31**, 328 (2020).
 - ²³Pritam, A. Arya and A. L. Sharma, Selection of best composition of Na⁺ ion conducting PEO-PEI blend solid polymer electrolyte based on structural, electrical, and dielectric spectroscopic analysis, *Ionics* **26**, 745 (2020).
 - ²⁴M. Sadiq, M. M. H. Raza, T. Murtaza, M. Zulfeqar and J. Ali, Sodium ion-conducting polyvinylpyrrolidone (PVP)/polyvinyl alcohol (PVA) blend electrolyte films, *J. Electron. Mater.* **50**, 403 (2021).
 - ²⁵K. K. Ganta, V. R. Jeedi, K. V. Kumar and E. L. Narsaiah, Preparation, characterization and impedance spectroscopic studies of Na⁺ ion conducting PEO + PVDF-blended polymer electrolytes, *Int. J. Polym. Anal. Charact.* **26**, 130 (2021).
 - ²⁶J. Hu, W. Wang, B. Zhou, Y. Feng, X. Xie and Z. Xue, Poly (ethylene oxide)-based composite polymer electrolytes embedding with ionic bond modified nanoparticles for all-solid-state lithium-ion battery, *J. Membr. Sci.* **575**, 200 (2019).
 - ²⁷S. Jayanthi and B. Sundaresan, Influence of nano SrTiO₃ and ultrasonic irradiation on the properties of polymer blend electrolytes, *Polym. Plast. Technol. Mater.* **59**, 2050 (2020).
 - ²⁸Pritam, A. Arya and A. L. Sharma, *Recent Research Trends in Energy Storage Devices*, eds. Y. Sharma, G. D. Varma, A. Mukhopadhyay and V. Thangadurai, Chap. 14 (Springer Nature, Singapore, 2021), pp. 115–124.
 - ²⁹S. Sharma, D. Pathak, R. Kumar, V. Sharma, N. Arora, S. Kaur and V. Sharma, *Nano Tools and Devices for Enhanced Renewable Energy*, Micro and Nano Technologies, eds. S. Devasahayam and C. M. Hussain, Chap. 2 (Elsevier Science and Technology, 2021), pp. 27–40.
 - ³⁰C. Devi, J. Gellanki, H. Pettersson, S. Kumar, High sodium ionic conductivity in PEO/PVP solid polymer electrolytes with InAs nanowire fillers, *Sci. Rep.* **11**, 20180 (2021).
 - ³¹L. T. Khoon, N. A. Dzulkurnain and A. Ahmad, *Synthetic and Natural Nanofillers in Polymer Composites, Properties and Applications*, Woodhead Publishing Series in Composites Science and Engineering, eds. N. M. Nurazzi, R. A. Ilyas, S. M. Sapuan and A. Khalina, Chap. 14 (Woodhead Publishing-Elsevier Ltd., 2023), pp. 313–329.
 - ³²S. N. F. Yusuf and A. K. Arof, *Polymer Electrolytes: Characterization Techniques and Energy Applications*, eds. T. Winie, A. K. Arof and S. Thomas, Chap. 6 (Wiley-VCH, Weinheim, 2019), pp. 137–186.
 - ³³N. Boaretto, L. Meabe, M. Martinez-Ibañez, M. Armand and H. Zhang, Review — polymer electrolytes for rechargeable batteries: From nanocomposite to nanohybrid, *J. Electrochem. Soc.* **167**, 070524 (2020).
 - ³⁴Y. L. Ni'mah, M. Y. Cheng, J. H. Cheng, J. Rick and B. J. Hwang, Solid-state polymer nanocomposite electrolyte of TiO₂/PEO/NaClO₄ for sodium ion batteries, *J. Power Sources* **278**, 375 (2015).
 - ³⁵S. Jayanthi and B. Sundaresan, Effect of ultrasonic irradiation and TiO₂ on the determination of electrical and dielectric properties of PEO-P(VdF-HFP)-LiClO₄-based nanocomposite polymer blend electrolytes, *Ionics* **21**, 705 (2015).
 - ³⁶S. Jayanthi, K. Kulasekarapandian, A. Arulsankar, K. Sankaranarayanan and B. Sundaresan, Influence of nano-sized TiO₂ on the structural, electrical, and morphological properties of polymer-blend electrolytes PEO-PVC-LiClO₄, *J. Compos. Mater.* **49**, 1035 (2015).
 - ³⁷W. Wang and P. Alexandridis, Composite polymer electrolytes: Nanoparticles affect structure and properties, *Polymers* **8**, 387 (2016).
 - ³⁸A. Arya and A. L. Sharma, Structural, microstructural and electrochemical properties of dispersed-type polymer nanocomposite films, *J. Phys. D: Appl. Phys.* **51**, 045504, (2018).
 - ³⁹R. J. Sengwa, S. Choudhary and P. Dhatwarwal, Nonlinear optical and dielectric properties of TiO₂ nanoparticles incorporated PEO/PVP blend matrix based multifunctional polymer nanocomposites, *J. Mater. Sci.: Mater. Electron.* **30**, 12275 (2019).
 - ⁴⁰D. Nunes, A. Pimentel, L. Santos, P. Barquinha, L. Pereira, E. Fortunato and R. Martins, *Metal Oxide Nanostructures: Synthesis, Properties and Applications*, Chap. 7 (Elsevier, Amsterdam, 2019), pp. 235–282.

- ⁴¹H. Verma, K. Mishra and D. K. Rai, Sodium ion conducting nanocomposite polymer electrolyte membrane for sodium ion batteries, *J. Solid State Electrochem.* **24**, 521 (2020).
- ⁴²A. Chandra, A. Chandra, R. S. Dhundhel, A. Jain and A. Bhatt, Preparation and ion transport properties of a new TiO₂ dispersed sodium ion conducting nanocomposite polymer electrolytes, *Russ. J. Electrochem.* **57**, 375 (2021).
- ⁴³K. K. Ganta, V. R. Jeedi, K. V. Kumar, Y. Mallaiah and E. L. Narsaiah, Effect of TiO₂ nano-filler on electrical properties of Na⁺ ion conducting PEO/PVDF based blended polymer electrolyte, *J. Inorg. Organomet. Polym.* **31**, 3430 (2021).
- ⁴⁴R. Sharma, A. Verma, A. Chandra and A. Chandra, Ion transport property studies of a new TiO₂ dispersed Na⁺ ion conducting nanocomposite polymer electrolytes, *Mater. Today: Proc.* **49**, 2168 (2022).
- ⁴⁵S. Jayanthi, S. Shenbagavalli, M. Muthuvinayagam and B. Sundaresan, Effect of nano TiO₂ on the transport, structural and thermal properties of PEMA-NaI solid polymer electrolytes for energy storage devices, *Mater. Sci. Eng. B* **285**, 115942 (2022).
- ⁴⁶N. Kumar, D. K. Sahu and Y. K. Mahipal, Effect of TiO₂ on ion transport properties and dielectric relaxation of sodium ion-conducting novel PEO/PAN-blended solid polymer electrolyte, *J. Mater. Res.* **38**, 2506 (2023).
- ⁴⁷M. Forsyth, D. R. MacFarlane, A. Best, J. Adebahr, P. Jacobsson and A. J. Hill, The effect of nano-particle TiO₂ fillers on structure and transport in polymer electrolytes, *Solid State Ion.* **147**, 203 (2002).
- ⁴⁸C. W. Lin, C. L. Hung, M. Venkateswarlu and B. J. Hwang, Influence of TiO₂ nano-particles on the transport properties of composite polymer electrolyte for lithium-ion batteries, *J. Power Sources* **146**, 397 (2005).
- ⁴⁹A. C. Bloise, J. P. Donoso, C. J. Magon, A. V. Rosario and E. C. Pereira, NMR and conductivity study of PEO-based composite polymer electrolytes, *Electrochim. Acta* **48**, 2239 (2003).
- ⁵⁰H. K. Koduru, K. K. Kondamareddy, M. T. Iliev, Y. G. Marinov, G. B. Hadjichristov, D. Karashanova and N. Scaramuzza, Synergistic effect of TiO₂ nano filler additives on conductivity and dielectric properties of PEO/PVP nanocomposite electrolytes for electrochemical cell applications, *J. Phys. Conf. Ser.* **780**, 012006 (2017).
- ⁵¹Y. G. Marinov, G. B. Hadjichristov, T. E. Vlahov, H. K. Koduru and N. Scaramuzza, Electrochemical impedance and dielectric spectroscopy study of TiO₂-nanofilled PEO/PVP/NaIO₄ ionic polymer electrolytes, *Bulg. Chem. Commun.* **52**, 57 (2020).
- ⁵²M. T. Iliev, H. K. Koduru, L. Marino, Y. G. Marinov, D. Karashanova and N. Scaramuzza, Studies on conductivity and dielectric properties of PEO/PVP nanocomposite electrolytes for energy storage device applications, *Bulg. Chem. Commun.* **53**, 5 (2021).
- ⁵³T. E. Vlahov, G. B. Hadjichristov, Y. G. Marinov and N. Scaramuzza, Ion conductivity of nanocomposite solid polymer electrolyte PEO-PVP-NaIO₄ with added TiO₂ nanoparticles, *C. R. Acad. Bulg. Sci.* **75**, 349 (2022).
- ⁵⁴T. Vlahov, Y. Marinov, G. Hadjichristov and N. Scaramuzza, Electrical conductivity properties of solid polymer electrolytes PEO-PVP-NaIO₄ filled with TiO₂ nanoparticles, *C. R. Acad. Bulg. Sci.* **75**, 804 (2022).
- ⁵⁵H. K. Koduru, L. Marino, F. Scarpelli, A. G. Petrov, Y. G. Marinov, G. B. Hadjichristov, M. T. Iliev and N. Scaramuzza, Structural and dielectric properties of NaIO₄-complexed PEO/PVP blended solid polymer electrolytes, *Curr. Appl. Phys.* **17**, 1518 (2017).
- ⁵⁶M. Rezaee, S. M. Mousavi Khoei and K. H. Liu, The role of brookite in mechanical activation of anatase-to-rutile transformation of nanocrystalline TiO₂: An XRD and Raman spectroscopy investigation, *CrystEngComm.* **13**, 5055 (2011).
- ⁵⁷F. E. Bailey, Jr. and J. V. Koleske, *Poly(Ethylene Oxide)* (Academic Press, New York, 1976).
- ⁵⁸R. C. Agrawal, S. A. Hashmi and G. P. Pandey, Electrochemical cell performance studies on all-solid-state battery using nano-composite polymer electrolyte membrane, *Ionics* **13**, 295 (2007).
- ⁵⁹A. Arya and A. L. Sharma, Insights into the use of polyethylene oxide in energy storage/conversion devices: A critical review, *J. Phys. D. Appl. Phys.* **50**, 443002 (2017).
- ⁶⁰Y. Takahashi and H. Tadokoro, Structural studies of polyethers, $-(\text{CH}_2)_m\text{-O})_n$. X. Crystal structure of poly(ethylene oxide), *Macromolecules* **6**, 672 (1973).
- ⁶¹H. K. Koduru, M. T. Iliev, K. K. Kondamareddy, D. Karashanova, T. Vlahov, X. Z. Zhao and N. Scaramuzza, Investigations on Poly(ethylene oxide) (PEO)-blend based solid polymer electrolytes for sodium ion batteries, *J. Phys. Conf. Ser.* **764**, 012006 (2016).
- ⁶²G. B. Hadjichristov, Tz. E. Ivanov, Y. G. Marinov, H. K. Koduru and N. Scaramuzza, PEO-PVP-NaIO₄ ion-conducting polymer electrolyte: Inspection for ionic space charge polarization and charge trapping, *Phys. Status Solidi (A): Appl. Mater. Sci.* **216**, 1800739 (2019).
- ⁶³C. H. Porter and R. H. Boyd, Dielectric study of effects of melting on molecular relaxation in poly(ethylene oxide) and polyoxymethylene, *Macromolecules* **4**, 589 (1971).
- ⁶⁴S. Marinel, D. H. Choi, R. Heuguet, D. Agrawal and M. Lanagan, Broadband dielectric characterization of TiO₂ ceramics sintered through microwave and conventional processes, *Ceram. Int.* **39**, 299 (2013).
- ⁶⁵A. Wypych, I. Bobowska, M. Tracz, A. Opasinska, S. Kadlubowski, A. K. Kaliszewska, J. Grobelny and P. Wojciechowski, Dielectric properties and characterisation of Titanium Dioxide obtained by different chemistry methods, *J. Nanomater.* **2014**, 124814 (2014).
- ⁶⁶G. Polizos, E. Tuncer, V. Tomer, I. Sauers, C. A. Randall and E. Manias, *Nanoscale Spectroscopy with Applications*, ed. S. M. Musa, Chap. 3 (CRC Press, Boca Raton, 2013), pp. 93–130.
- ⁶⁷R. Kohlrausch, Theorie des Elektrischen Rückstandes in der Leidener Flasche, *Prog. Ann. Phys.* **91**, 179 (1854).
- ⁶⁸G. Williams and D. C. Watts, Non-symmetrical dielectric relaxation behaviour arising from a simple empirical decay function, *Trans. Faraday Soc.* **66**, 80 (1970).
- ⁶⁹D. P. Almond and A. R. West, Mobile ion concentrations in solid electrolytes from an analysis of a.c. conductivity, *Solid State Ionics* **9**, 277 (1983).
- ⁷⁰V. Alzari, D. Nuvoli, V. Sanna, T. Caruso, S. Marino and N. Scaramuzza, Study of polymeric nanocomposites prepared by inserting graphene and or Ag, Au and ZnO nanoparticles in a TEGDA polymer matrix, by means of the use of dielectric spectroscopy, *AIP Adv.* **6**, 35005 (2016).
- ⁷¹P. Pal and A. Ghosh, Investigation of ionic conductivity and relaxation in plasticized PMMA-LiClO₄ solid polymer electrolytes, *Solid State Ion.* **319**, 117 (2018).
- ⁷²F. Schönhalz and A. Kremer, *Broadband Dielectric Spectroscopy* (Springer, Berlin, 2003).

- ⁷³A. Arya and A. L. Sharma, Structural, electrical properties and dielectric relaxations in Na⁺-ion-conducting solid polymer electrolyte, *J. Phys. Condens. Matter* **30**, 165402 (2018).
- ⁷⁴A. Arya, N. G. Saykar and A. L. Sharma, Impact of shape (nanofiller vs. nanorod) of TiO₂ nanoparticle on free-standing solid polymeric separator for energy storage/conversion devices, *J. Appl. Polym. Sci.* **136**, 47361 (2019).
- ⁷⁵H. K. Koduru, F. Scarpelli, Y. G. Marinov, G. B. Hadjichristov, P. M. Rafailov, I. K. Miloushev, A. G. Petrov, N. Godbert, L. Bruno and N. Scaramuzza, Characterization of PEO/PVP/GO nanocomposite solid polymer electrolyte membranes: Microstructural, thermo-mechanical, and conductivity properties, *Ionics* **24**, 3459 (2018).
- ⁷⁶H. K. Koduru, L. Bruno, Y. G. Marinov, G. B. Hadjichristov and N. Scaramuzza, Mechanical and sodium ion conductivity properties of graphene oxide-incorporated nanocomposite polymer electrolyte membranes, *J. Solid State Electrochem.* **23**, 2707 (2019).
- ⁷⁷I. Sevostianov, A. Trofimov, J. Merodio, R. Penta and R. Rodriguez-Ramos, Connection between electrical conductivity and diffusion coefficient of a conductive porous material filled with electrolyte, *Int. J. Eng. Sci.* **121**, 108 (2017).